2022 19th International Conference on Electrical Engineering, Computing Science and Automatic Control (CCE). Mexico City, Mexico. November 9-11, 2022

Effect of the oxidation degree on the bandgap of graphene oxides by Tour method

Francisco J. Cano
Nanociencia y Nanotecnología, CINVESTAV, México
IMMM, Le Mans Université, France
franciscojavier.cano@cinvestav.edu.mx
francisco.gomez_cano.etu@univ-lemans.fr

O. Reyes-Vallejo
Ingeniería eléctrica (SEES), CINVESTAV- IPN, México
odin.reyes.v@cinvestav.mx

José Juan Díaz
Nanociencias y Nanotecnología, CINVESTAV- IPN, México
jose.diaz@cinvestav.mx

S. Velumani
Ingeniería eléctrica (SEES), CINVESTAV- IPN, México
velu@cinvestav.mx

A. Kassiba
IMMM, Le Mans Université, France
abdelhadi.kassiba@univ-lemans.fr

Abstract
In this work graphene oxides (GOs) were synthesized by the tour method. The oxidation degree of GOs was varied using different dosages of $KMnO_4$ during the synthesis (0.5, 3, and 6 g). By X-ray diffraction (XRD) and X-ray photoelectron spectroscopy (XPS), we quantitatively determined the oxidation degree of the materials (4.1, 49.5, and 53.9%). In addition, bandgaps ranging from 0.8 to 2.18 eV were calculated, thus verifying the dependence of the bandgap on the oxidation degree. With this work, we demonstrate that by the tour method it is possible to synthesize and control the oxidation degree in the GOs, in such a way that we can change the nature of the material from semimetallic to semiconducting with the modification of its bandgap. The study of our GOs was complemented with FT-IR spectroscopy and Raman spectroscopy.

Keywords: Graphene oxide, bandgap, tour method, oxidation degree

1. Introduction

Two-dimensional materials have emerged as promising platforms for investigating innovative and unusual features not seen in conventional materials. Due to its exceptional electrical, optical, mechanical, and thermal properties for a wide range of applications, carbon-based materials have been widely researched [1]. One of them is graphene oxide (GO) [2, 3]. GO is a carbon nanomaterial obtained by oxidation of graphene, which can be mass-produced by exfoliation of graphite [4]. As a derivative of graphene, graphene oxide is described as a monolayer sheet of sp^2 and sp^3 hybridized carbons, where the graphene-like skeleton is interrupted by various oxidative functionalities on the basal plane and edges [5]. These functionalities (hydroxyl, carbonyl, epoxide, carboxylic) favor exfoliation because they increase the distance between the graphene layers, facilitating the separation of the layers by ultrasound application [6]. Several theoretical-experimental works have reported the variation of GO properties depending on the oxidation degree they present [7-9], having then the possibility of adapting their properties according to their intended application. One of them is the bandgap, which is a physical property that determines whether a material has a conductive, insulating, or semiconducting nature [10]. For this purpose, there are different synthesis methods for the preparation of GOs with different oxidation degrees, such as Brodie [11], Staudenmaier [12], and the Hummer method [13], mainly.

We synthesized GOs with three different oxidation degrees (GO_1, GO_2, and GO_3) by the tour method. To the best of our knowledge, the tour method has been referenced in several papers as a reliable method for the synthesis and control of graphene [14], however, we have not found precedents of research groups that have analyzed the different oxidation degrees in GO by such a method. Bandgaps were calculated for our materials, observing a clear dependence on the amount of oxidant ($KMnO_4$) added during the synthesis process. In addition, with the help of XRD and XPS, the oxidation degree was quantitatively determined for each of them. The oxidation degrees were also observed qualitatively by Fourier transform infrared spectroscopy (FTIR) and Raman spectroscopy.

2. Materials and methods

2.1. GO by the Tour method

Our materials were made by mixing 43.2 mL of H_2SO_4 (sulfuric acid ACS reagent, 95.0%-98.0%) and 4.8 mL H_3PO_4 (ortho-phosphoric acid, 85%) in a 9:1(v/v) ratio. The acid mixture is poured into 1 g of graphite powder and stirred continuously for 3 hours in a cold bath at 4°C. The oxidation degree was varied using 0.5 g, 3 g, and 6 g of $KMnO_4$, respectively. After 2 hours, a dropwise addition of 12 mL of analytical grade H_2O_2 (30% w/w) and 13 mL of HCl (36.5%-38.0%) was made. To stop the process, distilled water was added to the mixture after 30 min. The exfoliation process was then carried out for 30 min by using sonication. Through centrifugation at 4000 rpm for 30 min, a washing process was repeated until the residual liquid attained a pH of 7. Finally, the resulting pastes were dried for 18 hours at 65°, obtaining GO powders with three different degrees of oxidation.

2.2. Characterization

2.2.1. Infrared spectroscopy by Fourier Transform (FTIR)

Analysis of FTIR was performed on a Perkin-Elmer Frontier FTIR instrument using a diamond ATR accessory in the 1200-3400 cm^{-1} range with a resolution of 4 cm^{-1}.

2.2.2. X-ray diffraction (XRD)

X-ray diffraction (XRD) provides strong evidence of the oxidation reaction and modification of the crystal structure of the initial graphite. The diffraction pattern was performed using a D2 PHASER Bruker diffractometer under Cu-Kα radiation

978-1-6654-5508-4/22/$31.00 ©2022 IEEE

(λ=1.54056 Å), using a voltage of 40 kV and a current of 30 mA. The scanning range for GOs was done at 2θ from 8°-60°, with a scanning speed of 0.02°/min. The Bragg equation [15] was applied to the reflection (001) to estimate the average d_{001} distance between graphene layers.

$$2d_{001}\, sin\theta = n\lambda \qquad (Eq.\ 1)$$

2.2.3. *Raman spectroscopy*

The Raman spectroscopy analysis was performed using an NT-MDT Ntegra Spectrometer. The spectra were obtained in the range of 800 to 1800 cm^{-1} with a total of 32 scans per spectrum, an opening of 25 m for slit, and the use of a laser of 532 nm as the excitation.

2.2.4. *X-ray photoelectron spectroscopy (XPS)*

XPS spectra of the GOs were taken on a PHI Versa Probe II spectrometer using monochromatic AlKα radiation with an energy of 1486.6 eV. The scanning range was 278–300 eV. Additionally, we quantitatively obtained the oxidation degree in this work using the intensities I_{sp2} and I_{sp3} by XPS and the intensities of graphite ($I_{Graphite}$) and GO (I_{GO}), thus verifying the direct relationship of the oxidation degree as a function of the amount of $KMnO_4$ added during the synthesis process, as reported by Yan, H. *et al* (2014) [16].

$$OD(\%) = \left(\frac{I_{sp^3}}{I_{sp^3}+I_{sp^2}}\right)\left(\frac{I_{GO}}{I_{GO}+I_{Graphite}}\right)(100) \qquad (Eq.\ 2)$$

2.2.5. *UV-Vis Spectroscopy*

Diffuse reflectance spectrum was recorded on a JASCO spectrometer model V-670 equipped with integration sphere model IJN727. The bandgap was calculated by linear extrapolation of Tauc plots (equation 3) [17] using optical absorbance data plotted appropriately concerning energy.

$$(\alpha h\nu)^{1/n} = k(h\nu - E_g) \qquad (Eq.\ 3)$$

where $\alpha h\nu$ is the photon energy, E_g is the bandgap, n is the nature of transmission and A is the slope of the Tauc plot in the linear region. The exponent's value indicates the type of electronic transition, whether it is direct or indirect, permissible or disallowed. However, it was not possible to distinguish between direct and indirect bandgaps in the case of our materials.

3. Results and discussion

Figure 1 shows the FT-IR analysis of the precursor graphite and the synthesized GOs. Intense peaks in GOs samples were observed at wavelengths of ≈3302 cm^{-1} due to the presence of the O-H bond (hydroxyl group) and ≈3200 cm^{-1} due to the hydrogen-bonded water (H-O-H) stretching. The -C=O stretching (carboxyl group) appeared at ≈1722 cm^{-1} [18], while the C-OH stretching appeared at ≈1373 cm^{-1} and epoxy is observed at ≈1200 cm^{-1}, respectively, while the peak around ≈1556 cm^{-1} was attributed to the C=C bonds of the non-oxidized domains [19]. These peaks did not appear in the graphite spectrum, indicating that the chemical oxidation process introduces many oxygen-containing functional groups, and these groups must include -COOH and C=O located at the edge of the sheet, -OH, and epoxy C-O over the basal planes of the GO sheet [20].

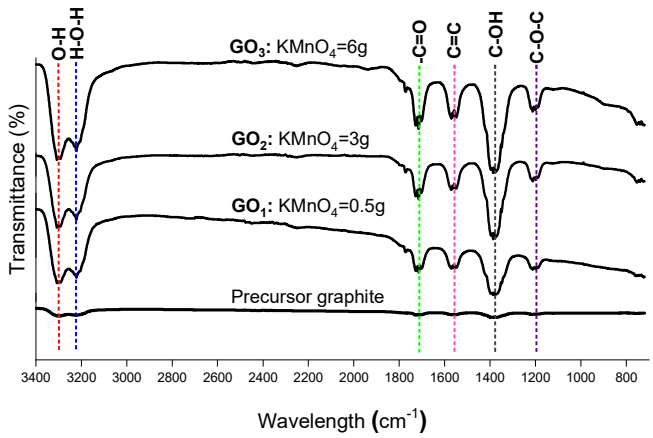

Figure 1. *FT-IR of the precursor graphite and GOs with different oxidation degrees.*

The synthesized GOs were analyzed by XRD to observe the evolution of the main peaks as a function of the amount of $KMnO_4$ added during the synthesis process (figure 2a). In the diffraction pattern, graphite shows a characteristic peak at 2θ=26.20°, which corresponds to the plane (002). After the introduction of oxygenated functional groups, the intensity of the graphite peak is reduced until it disappears, but at the same time, a new broad peak appears at 2θ=13.04°, corresponding to the plane (001) of the GOs. In GO_2 the peak of the plane (001) is more intense and is shifted to 2θ=9.51°. While in the GO_3, the peak is defined and more intense, shifting to 2θ=9.58°. This confirms that the oxidation of graphite has been successfully carried out and it is at the same time coincident with previously reported work [21]. The peak of the plane (001) represents the existence of an intercalated H_2O molecule and an oxygenated functional group that is strongly bound to it [22, 23]. The variation in the interplanar spacing of GO results from the variation in the oxidation degree in graphite and is proportional to the oxygen content [24]. Figure 2b shows that the interplanar distance is larger for GOs concerning the precursor graphite and increases with the higher oxidation degree due to the intercalation of water molecules and the formation of epoxy, hydroxyl, carbonyl, and carboxyl functional groups in the basal plane of the graphite [14, 25, 26].

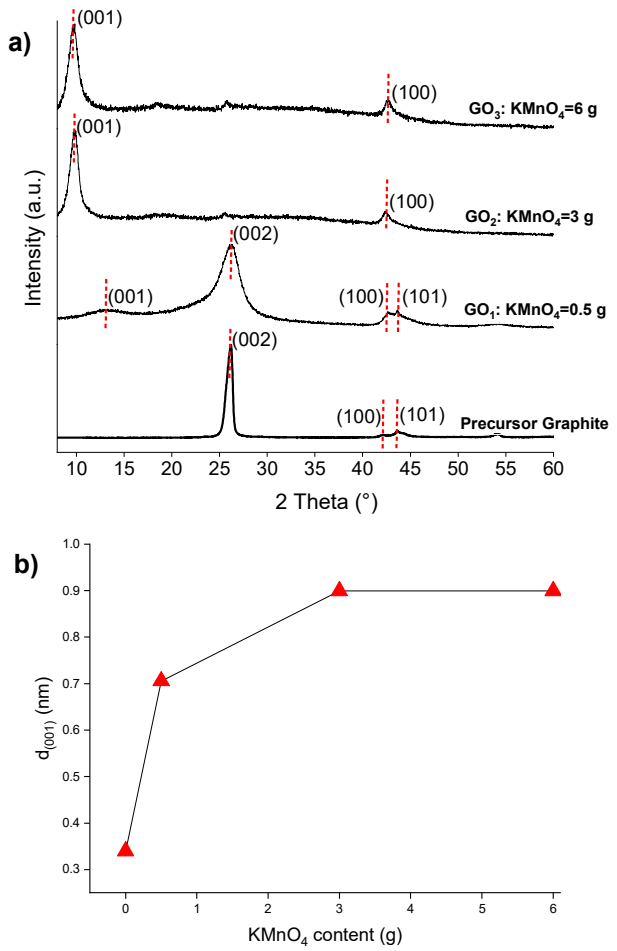

Figure 2. *Graphite precursor and graphene oxides with different doses of $KMnO_4$ (a) X-ray diffraction spectra, (b) interplanar distance (001) plane.*

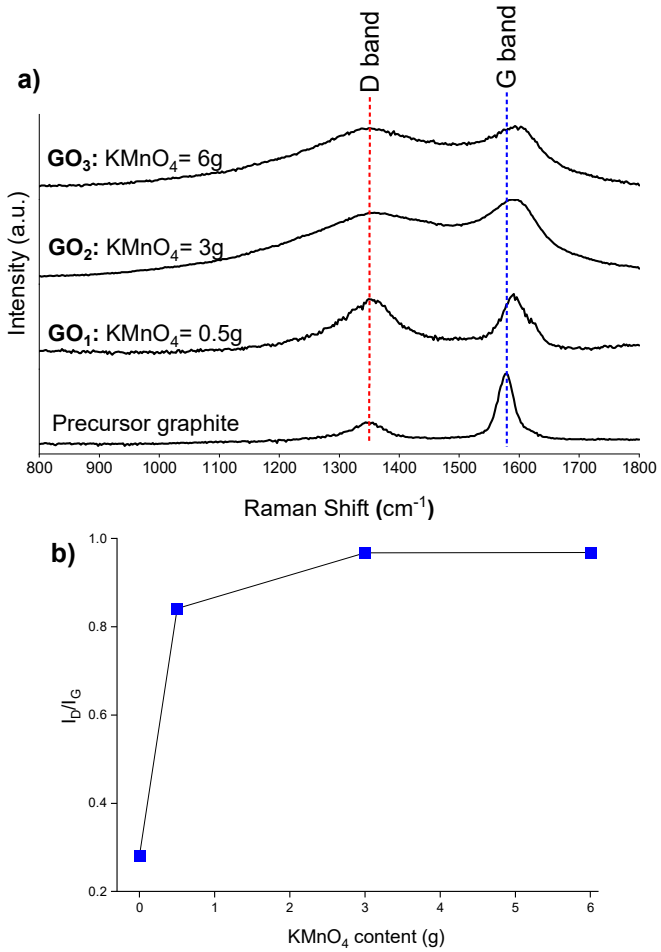

Figure 3. *Graphite precursor and graphene oxides with different doses of $KMnO_4$ (a) Raman spectra, (b) I_D/I_G ratio.*

The Raman spectra for each GO and the graphite present two bands as shown in figure 3a. In graphite, the D band is located at 1351 cm^{-1} and is associated with the order/disorder in the lattice of the material, while the G band located at 1579 cm^{-1} is caused by the stretching of the bonds in the plane of the sp^2 carbon atom pairs [27, 28]. In GO_1 the G-band shifted to 1588 cm^{-1}; in GO_2 the band moved to 1592 cm^{-1} and finally in GO_3 to 1601 cm^{-1}, with such a shift suggesting a higher oxidation degree in the material [29, 30]. On the other hand, an increase in the number of defects in the graphitic network results in a gradual increase in the intensity of the D peak concerning the G peak, as observed in figure 3b. Graphite presented an I_D/I_G ratio of 0.2804, suggesting a material with a high degree of order, while GO_1, GO_2, and GO_3 showed ratios of 0.8411, 0.9675, and 0.9685, respectively, where the degree of the disorder increased significantly. The ratio of I_D/I_G intensities has been used to indicate the average sp^2 domain size in graphitic sheets, such that its increase in GOs compared to graphite, indicates that the sp^2 states are broken and many sp^3 hybridized carbon atoms are induced by oxygen-containing functional groups, thus causing the isolation or reduction of the average size of sp^2 domains, due to the incorporation of $KMnO_4$ during synthesis [6, 29, 30].

The GOs were further analyzed by XPS as shown in figure 4. Four peaks were deconvoluted for the carbon 1s spectrum obtained from the GO corresponding to the following functional groups: C=C/C-C in aromatic rings, C epoxy (C-O), C carbonyl (C=O), and C carboxyl (-COOH) [18, 31, 32]. Overall, the spectra in figure 4 showed an intense band at ~284.8 eV attributed to C=C (sp^2) bonds and a less intense band at ~286.9 eV attributed to sp^3 hybridization [33-36]. GO_1 (figure 4a) showed a band at 284.8 eV attributed to aromatic rings (C=C/C-C) with 51.2%. Likewise, the presence of C-epoxy (C-O) at 286.8 eV with 27.7% and C-Carbonyl (C=O) at 287.6 eV with 21.1% is also observed. The presence of two types of oxygenated functional groups is related to the $KMnO_4$: graphite ratio used for the synthesis of GO_1 since it was not sufficient to oxidize the epoxy or carbonyl groups to carboxylic [37]. In GO_2 (figure 4b), it showed the presence of 48.1% aromatic rings (C=C/C-C) at 284.8 eV; while the oxygenated groups found were 17.5% epoxides (C-O) at 286.7 eV, 19.1% Carbonyls (C=O) at 287.1 eV and 15.3% Carboxyl groups (-COOH) at 288.2 eV. Finally, GO_3 (figure 4c) presented 46.9% aromatic rings (C=C/C-C) at 284.7 eV and 15.6% (C-O), 18.6% (C=O) and 18.9% (-COOH) at 286.6 eV, 287.1 eV and 288.1 eV, respectively.

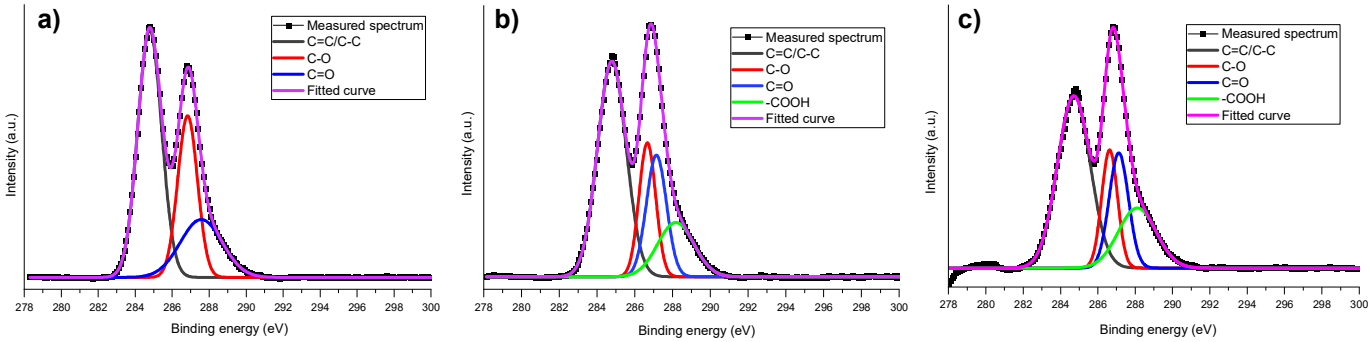

Figure 4. *XPS spectra (C1s) and deconvolutions were obtained for GO (a) GO_1, (b) GO_2, and (c) GO_3.*

Table I presents the quantification of the functional groups for GO_1, GO_2, and GO_3, obtained from the calculation of the areas under the curve. It was observed that as the oxidation degree increased so did the concentration of functional groups, this coincident with the increase of sp^3 states obtained by Raman spectroscopy. The C=C bonds come from the graphitic structure, the C-O was attributed to the C-O-C and C-OH functional groups, while the C=O was also assigned to the COOH functional groups [47]. As can be seen, the predominant functional groups obtained, were C-OH and C-O-C in contrast to C=O and COOH, being coincident with previous results reported in the literature. Additionally, using equation 2 reported by Yan, H. *et al.* (2014) [16] we quantitatively obtained the oxidation degree for GO_1, GO_2, and GO_3.

Table I. *Quantification of functional groups in GO_1, GO_2, and GO_3 by XPS.*

Material	Functional group					$KMnO_4$ (g)	% OD
		C=C/C-C	C-O	C=O	-COOH		
GO_1	Position (eV)	284.8	286.8	287.6	---	0.5	4.10%
	Area (%)	51.2%	27.7%	21.1%	---		
GO_2	Position (eV)	284.8	286.7	287.1	288.2	3	49.50%
	Area (%)	48.1%	17.5%	19.1%	15.3%		
GO_3	Position (eV)	284.7	286.6	287.1	288.1	6	53.90%
	Area (%)	46.9%	15.6%	18.6%	18.9%		

In graphene (G) previous work has reported a bandgap of 0 eV [38] because the valence and conduction bands touch at two points in the reciprocal space known as *K* and *K'*, whose corresponding energies are exactly at the Fermi energy. Since there is no space between the two bands, electrons can safely jump from the valence band to the conduction band only through that point [1]. The electrons in this material move relatively freely, so they do so almost without causing collisions with the crystal lattice, even at room temperature. This extraordinary electronic structure gives G unique physical properties due to its linear dispersion relation, high symmetry, and degree of freedom. The presence of the extensive delocalized π electron cloud and the fast charge carrier dynamics derived from its bandgap structure is responsible for the ballistic transport observed in G [1, 39]. Recent studies have shown that the zero bandgaps in G is a consequence of the identical environment possessed by the two atomic sublattices that compose it, suggesting that breaking this lateral in-plane symmetry either structurally or by chemical modifications could produce a bandgap in G [40, 41], as occurs in GOs.

The bandgap in figure 5 was determined with the help of Tauc plots with linear extrapolation (equation 3). Due to the amorphous nature and non-uniform oxidation levels of the GO films, a sharp adsorption edge was not obtained in the Tauc plot [53]. We observed the following bandgap ranges: GO_1 (0.87-0.95 eV), GO_2 (1.15-1.57 eV), and GO_3 (1.25-2.18 eV), observing a gradual increase as a function of the oxidation degree. In GOs, due to many functional groups [42], the symmetry of the hexagonal lattice plane is broken and many of the carbon atoms in the lattice change from having sp^2 to sp^3 hybridizations; therefore, the generated bandgap is so large that the material becomes a semiconductor or an electrical insulator.

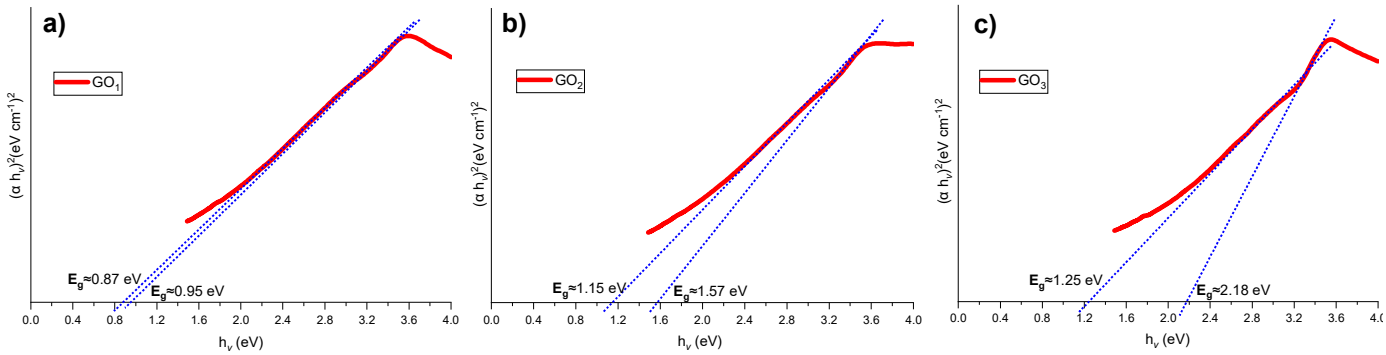

Figure 5. *Tauc plot for calculating the bandgap of (a) GO_1, (b) GO_2, and (c) GO_3.*

Table II shows some theoretical-experimental values published in the literature supporting our results. From this study, we found that the bandgap in graphene oxides can be modified with the dosage of $KMnO_4$ during the synthesis process. This is important because the material can be tailored to a particular application, modifying its properties ranging from semi-metallic to semiconducting and/or insulating [43-46].

Table II. *Bandgap values for GOs reported in the literature*

Oxidation degree (%)	Bandgap range (eV)	References
4.10 to 5.39	0.6 eV to 2.44 eV	This work
Unspecified	3.6 eV	[48]
Unspecified	0.02 eV to 2 eV	[49]
Unspecified	1.4 eV to 3.3 eV	[50]
2.0	3.2 eV	[51]
6.25 to 5.0	0.109 eV to 3.004 eV	[9]
Unspecified	6.5 eV	[52]
1.7 to 5.0	0.944 eV to 2.659	[7]
Unspecified	3.89 eV	[8]

4. Conclusion

In this work, we have successfully synthesized graphene oxides (GOs) with different oxidation degrees by regulating the dosage in 0.5 g, 1 g, and 6 g $KMnO_4$ during the synthesis by the tour method. By using XRD and XPS we quantitatively determined the oxidation degree for the three GOs. The analyses performed allowed us to know how the material changes structurally as oxygen is gradually incorporated. Furthermore, with this study we proved that the bandgap of the GOs can be increased at higher oxidation degrees, going from semi-metallic to semiconducting. This opens the possibility of adapting their properties depending on the application to be used for or incorporating them into another material as part of a composite to improve their joint properties.

Acknowledgments

The authors acknowledge Ing. Miguel Ángel Avendaño Ibarra (Measurements by Raman spectroscopy), Ing. Miguel Ángel Luna Arias (Measurements by UV-Vis spectroscopy), and Ing. Álvaro Guzmán Campuzano (Technical support) from CINVESTAV-SEES department; M. en C. Alejandra Garcia Sotelo from Physics department from CINVESTAV-Zacatenco (Measurements by Raman spectroscopy). F. J. Cano acknowledges BE-UP language & coaching school for English Language grand. The authors acknowledge CONACYT for the doctoral scholarship awarded to F. J. Cano and the postdoctoral scholarship to Odín Reyes Vallejo.

References

[1] Neto, A. C., Guinea, F., Peres, N. M., Novoselov, K. S., & Geim, A. K. (2009). The electronic properties of graphene. *Reviews of modern physics*, 81(1), 109. https://doi.org/10.1103/RevModPhys.81.109

[2] Fan, L., Luo, C., Sun, M., Li, X., Lu, F., & Qiu, H. (2012). Preparation of novel magnetic chitosan/graphene oxide composite as effective adsorbents toward methylene blue. *Bioresource Technology*, 114, 703-706. https://doi.org/10.1016/j.biortech.2012.02.067

[3] Xu, J., Wang, L., & Zhu, Y. (2012). Decontamination of bisphenol A from aqueous solution by graphene adsorption. *Langmuir,* 28(22), 8418-8425. https://doi.org/10.1021/la301476p

[4] Chen, L., Li, N., Wen, Z., Zhang, L., Chen, Q., Chen, L., ... & Ci, L. (2018). Graphene oxide-based membrane intercalated by nanoparticles for high-performance nanofiltration application. *Chemical Engineering Journal*, 347, 12-18. https://doi.org/10.1016/j.cej.2018.04.069

[5] Wang, Y., Chen, X., Zhong, Y., Zhu, F., Loh, K. P., Dreyer, D. R., ... & Ruoff, R. S. (2010). The chemistry of graphene oxide. *Chem Soc Rev*, *39*, 228-240. https://doi.org/10.1039/B917103G

[6] Stankovich, S., Piner, R. D., Nguyen, S. T., & Ruoff, R. S. (2006). Synthesis and exfoliation of isocyanate-treated graphene oxide nanoplatelets. *Carbon*, 44(15), 3342-3347. https://doi.org/10.1016/j.carbon.2006.06.004

[7] Jin, Y., Zheng, Y., Podkolzin, S. G., & Lee, W. (2020). The bandgap of reduced graphene oxide tuned by controlling functional groups. *Journal of Materials Chemistry C*, 8(14), 4885-4894. https://doi.org/10.1039/C9TC07063J

[8] Gupta, V., Sharma, N., Singh, U., Arif, M., & Singh, A. (2017). Higher oxidation level in graphene oxide. *Optik, 143*, 115-124. https://doi.org/10.1016/j.ijleo.2017.05.100

[9] Zhou, X., Zhang, J., Wu, H., Yang, H., Zhang, J., & Guo, S. (2011). Reducing graphene oxide via hydroxylamine: a simple and efficient route to graphene. *The Journal of Physical Chemistry C*, 115(24), 11957-11961. https://doi.org/10.1021/jp202575j

[10] Chaves, A., Azadani, J. G., Alsalman, H., Da Costa, D. R., Frisenda, R., Chaves, A. J., ... & Low, T. (2020). Bandgap engineering of two-dimensional semiconductor materials. *npj 2D Materials and Applications*, 4(1), 1-21. https://doi.org/10.1038/s41699-020-00162-4

[11] Brodie, B. C. (1859). XIII. On the atomic weight of graphite. *Philosophical transactions of the Royal Society of London*, (149), 249-259. https://doi.org/10.1098/rstl.1859.0013

[12] Staudenmaier, L. (1898). Verfahren zur darstellung der graphitsäure. *Berichte der deutschen chemischen Gesellschaft*, *31*(2), 1481-1487. https://doi.org/10.1002/cber.18980310237

[13] Hummers Jr, W. S., & Offeman, R. E. (1958). Preparation of graphitic oxide. *Journal of the american chemical society*, *80*(6), 1339-1339.

[14] Zainal, N., How, J. F., Choo, X. H., & Soon, C. F. (2020, September). Synthesis and characterization of graphene oxide (GO) and reduced graphene oxide (*r*GO) using Modified Tour's method for sensing device applications. In 2020 *IEEE Student Conference on Research and Development (SCOReD)* (pp. 385-390). IEEE. https://doi.org/10.1109/SCOReD50371.2020.9251005

[15] Elton, L. R. B., & Jackson, D. F. (1966). X-ray diffraction and the Bragg law. *American Journal of Physics*, 34(11), 1036-1038. https://doi.org/10.1119/1.1972439

[16] Yan, H., Tao, X., Yang, Z., Li, K., Yang, H., Li, A., & Cheng, R. (2014). Effects of the oxidation degree of graphene oxide on the adsorption of methylene blue. *Journal of hazardous materials*, 268, 191-198. https://doi.org/10.1016/j.jhazmat.2014.01.015

[17] Tauc, J., Grigorovici, R., & Vancu, A. Phys. (1996), *Status Solidi. B*, 15, 627-637.

[18] Xu, C., Shi, X., Ji, A., Shi, L., Zhou, C., & Cui, Y. (2015). Fabrication and characteristics of reduced graphene oxide produced with different green reductants. *PloS one*, 10(12), e0144842. https://doi.org/10.1371/journal.pone.0144842

[19] Guo, H. L., Wang, X. F., Qian, Q. Y., Wang, F. B., & Xia, X. H. (2009). A green approach to the synthesis of graphene nanosheets. *ACS nano*, 3(9), 2653-2659. https://doi.org/10.1021/nn900227d

[20] Sarkar, S. K., Raul, K. K., Pradhan, S. S., Basu, S., & Nayak, A. (2014). Magnetic properties of graphite oxide and reduced graphene oxide. *Physica E: Low-dimensional Systems and Nanostructures*, 64, 78-82. https://doi.org/10.1016/j.physe.2014.07.014

[21] Stobinski, L., Lesiak, B., Malolepszy, A., Mazurkiewicz, M., Mierzwa, B., Zemek, J., ... & Bieloshapka, I. (2014). Graphene oxide and reduced graphene oxide studied by the XRD, TEM and electron spectroscopy methods. *Journal of Electron Spectroscopy and Related Phenomena*, 195, 145-154. https://doi.org/10.1016/j.elspec.2014.07.003

[22] Pradhan, S. K., Xiao, B., Mishra, S., Killam, A., & Pradhan, A. K. (2016). Resistive switching behavior of reduced graphene oxide memory cells for low power nonvolatile device application. *Scientific reports*, 6(1), 1-9. https://doi.org/10.1038/srep26763

[23] Bo, Z., Shuai, X., Mao, S., Yang, H., Qian, J., Chen, J., ... & Cen, K. (2014). Green preparation of reduced graphene oxide for sensing and energy storage applications. *Scientific reports*, 4(1), 1-8. https://doi.org/10.1038/srep04684

[24] Drewniak, S., Muzyka, R., Stolarczyk, A., Pustelny, T., Kotyczka-Morańska, M., & Setkiewicz, M. (2016). Studies of reduced graphene

oxide and graphite oxide in the aspect of their possible application in gas sensors. *Sensors*, 16(1), 103. https://doi.org/10.3390/s16010103

[25] Zeng, F., Sun, Z., Sang, X., Diamond, D., Lau, K. T., Liu, X., & Su, D. S. (2011). In situ one-step electrochemical preparation of graphene oxide nanosheet-modified electrodes for biosensors. *ChemSusChem*, 4(11), 1587-1591. https://doi.org/10.1002/cssc.201100319

[26] Wojtoniszak, M., Chen, X., Kalenczuk, R. J., Wajda, A., Łapczuk, J., Kurzewski, M., ... & Borowiak-Palen, E. (2012). Synthesis, dispersion, and cytocompatibility of graphene oxide and reduced graphene oxide. *Colloids and Surfaces B: Biointerfaces*, 89, 79-85. https://doi.org/10.1016/j.colsurfb.2011.08.026

[27] Gurunathan, S., Han, J. W., Dayem, A. A., Eppakayala, V., Park, M. R., Kwon, D. N., & Kim, J. H. (2013). Antibacterial activity of dithiothreitol reduced graphene oxide. *Journal of Industrial and Engineering Chemistry*, 19(4), 1280-1288. https://doi.org/10.1016/j.jiec.2012.12.029

[28] Wang, C., Zhou, Y., Sun, L., Zhao, Q., Zhang, X., Wan, P., & Qiu, J. (2013). N/P-codoped thermally reduced graphene for high-performance supercapacitor applications. The Journal of Physical Chemistry C, 117(29), 14912-14919. Tuinstra, F., & Koenig, J. L. (1970). Raman spectrum of graphite. *The Journal of chemical physics*, 53(3), 1126-1130. https://doi.org/10.1021/jp4015959

[29] Ferrari, A. C., & Basko, D. M. (2013). Raman spectroscopy as a versatile tool for studying the properties of graphene. *Nature nanotechnology*, 8(4), 235-246. https://doi.org/10.1038/nnano.2013.46

[30] Kudin, K. N., Ozbas, B., Schniepp, H. C., Prud'Homme, R. K., Aksay, I. A., & Car, R. (2008). Raman spectra of graphite oxide and functionalized graphene sheets. *Nano letters*, 8(1), 36-41. https://doi.org/10.1021/nl071822y

[31] Stankovich, S., Piner, R. D., Chen, X., Wu, N., Nguyen, S. T., & Ruoff, R. S. (2006). Stable aqueous dispersions of graphitic nanoplatelets via the reduction of exfoliated graphite oxide in the presence of poly (sodium 4-styrenesulfonate). *Journal of Materials Chemistry*, 16(2), 155-158. https://doi.org/10.1039/B512799H

[32] Yang, D., Velamakanni, A., Bozoklu, G., Park, S., Stoller, M., Piner, R. D., ... & Ruoff, R. S. (2009). Chemical analysis of graphene oxide films after heat and chemical treatments by X-ray photoelectron and Micro-Raman spectroscopy. *Carbon*, 47(1), 145-152. https://doi.org/10.1016/j.carbon.2008.09.045

[33] Lau, W. M., Huang, L. J., Bello, I., 6ou, Y. M., & Lee, S. T. (1994). Modification of surface band bending of diamond by low energy argon and carbon ion bombardment. *Journal of applied physics*, 75(7), 3385-3391. https://doi.org/10.1063/1.357016

[34] Belton, D. N., & Schmieg, S. J. (1990). Electron spectroscopic identification of carbon species formed during diamond growth. Journal of Vacuum Science & Technology A: Vacuum, Surfaces, and Films, 8(3), 2353-2362. https://doi.org/10.1116/1.576697

[35] Reinke, P., Francz, G., Oelhafen, P., & Ullmann, J. (1996). Structural changes in diamond and amorphous carbon induced by low-energy ion irradiation. *Physical Review B*, 54(10), 7067. https://doi.org/10.1103/PhysRevB.54.7067

[36] Speranza, G., & Laidani, N. (2004). Measurement of the relative abundance of sp^2 and sp^3 hybridised atoms in carbon-based materials by XPS: a critical approach. Part I. *Diamond and related materials*, 13(3), 445-450. https://doi.org/10.1016/j.diamond.2003.11.077

[37] Seredych, M., Rossin, J. A., & Bandosz, T. J. (2011). Changes in graphite oxide texture and chemistry upon oxidation and reduction and their effect on adsorption of ammonia. *Carbon*, 49(13), 4392-4402. https://doi.org/10.1016/j.carbon.2011.06.032

[38] Meric, I., Han, M. Y., Young, A. F., Ozyilmaz, B., Kim, P., & Shepard, K. L. (2008). Current saturation in zero-bandgap, top-gated graphene field-effect transistors. *Nature nanotechnology, 3*(11), 654-659. https://doi.org/10.1038/nnano.2008.268

[39] Mayorov, A. S., Gorbachev, R. V., Morozov, S. V., Britnell, L., Jalil, R., Ponomarenko, L. A., ... & Geim, A. K. (2011). Micrometer-scale ballistic transport in encapsulated graphene at room temperature. *Nano letters*, 11(6), 2396-2399. https://doi.org/10.1021/nl200758b

[40] Li, Y., Zhao, Y., Cheng, H., Hu, Y., Shi, G., Dai, L., & Qu, L. (2012). Nitrogen-doped graphene quantum dots with oxygen-rich functional groups. *Journal of the American Chemical Society*, 134(1), 15-18. https://doi.org/10.1021/ja206030c

[41] Gokus, T., Nair, R. R., Bonetti, A., Bohmler, M., Lombardo, A., Novoselov, K. S., ... & Hartschuh, A. (2009). Making graphene luminescent by oxygen plasma treatment. *ACS nano*, 3(12), 3963-3968. https://doi.org/10.1021/nn9012753

[42] Eda, G., Mattevi, C., Yamaguchi, H., Kim, H., & Chhowalla, M. (2009). Insulator to semimetal transition in graphene oxide. *The Journal of Physical Chemistry C*, 113(35), 15768-15771. https://doi.org/10.1021/jp9051402

[43] Dreyer, D. R., Park, S., Bielawski, C. W., & Ruoff, R. S. (2010). The chemistry of graphene oxide. *Chemical society reviews*, 39(1), 228-240. https://doi.org/10.1039/B917103G

[44] Wang, Y., Wang, L., Wang, H. Y., Chen, Q. D., & Sun, H. B. (2019). Ultrafast Spectroscopic Study of Insulator–Semiconductor–Semimetal Transitions in Graphene Oxide and Its Reduced Derivatives. The *Journal of Physical Chemistry C*, 123(36), 22550-22555. https://doi.org/10.1021/acs.jpcc.9b03926

[45] Gómez-Navarro, C., Meyer, J. C., Sundaram, R. S., Chuvilin, A., Kurasch, S., Burghard, M., ... & Kaiser, U. (2010). Atomic structure of reduced graphene oxide. *Nano letters*, 10(4), 1144-1148. https://doi.org/10.1021/nl9031617

[46] IUPAC. Compendium of Chemical Terminology, 2nd ed. (the "Gold Book"). Compiled by A. D. McNaught and A. Wilkinson. *Blackwell Scientific Publications, Oxford* (1997). Online version (2019) created by S. J. Chalk. ISBN 0-9678550-9-8. https://doi.org/10.1351/goldbook

[47] Li, Z., Chen, F., Yuan, L., Liu, Y., Zhao, Y., Chai, Z., & Shi, W. (2012). Uranium (VI) adsorption on graphene oxide nanosheets from aqueous solutions. *Chemical engineering journal*, 210, 539-546. https://doi.org/10.1016/j.cej.2012.09.030

[48] Nourbakhsh, A., Cantoro, M., Vosch, T., Pourtois, G., Clemente, F., van der Veen, M. H., ... & Sels, B. F. (2010). Bandgap opening in oxygen plasma-treated graphene. *Nanotechnology*, 21(43), 435203. https://doi.org/10.1088/0957-4484/21/43/435203

[49] Shen, Y., Yang, S., Zhou, P., Sun, Q., Wang, P., Wan, L., ... & Zhang, D. W. (2013). Evolution of the bandgap and optical properties of graphene oxide with controllable reduction level. *Carbon*, 62, 157-164. https://doi.org/10.1016/j.carbon.2013.06.007

[50] Lian, K. Y., Ji, Y. F., Li, X. F., Jin, M. X., Ding, D. J., & Luo, Y. (2013). Big bandgap in highly reduced graphene oxides. *The Journal of Physical Chemistry C*, 117(12), 6049-6054. https://doi.org/10.1021/jp3118067

[51] Mkhoyan, K. A., Contryman, A. W., Silcox, J., Stewart, D. A., Eda, G., Mattevi, C., ... & Chhowalla, M. (2009). Atomic and electronic structure of graphene-oxide. *Nano letters*, 9(3), 1058-1063. https://doi.org/10.1021/nl8034256

[52] Lundie, M. J., Tomić, S., & Šljivančanin, Ž. (2014). Ab initio study of structural and electronic properties of partially reduced graphene oxide. *Physica Scripta*, 2014(T162), 014019. https://doi.org/10.1088/0031-8949/2014/T162/014019

[53] Kumar, P., Sain, B., & Jain, S. L. (2014). Photocatalytic reduction of carbon dioxide to methanol using a ruthenium trinuclear polyazine complex immobilized on graphene oxide under visible light irradiation. *Journal of Materials Chemistry A*, 2(29), 11246-11253. https://doi.org/10.1039/C4TA01494D